DUST CONDENSATION IN THE EJECTA OF SN 1987A

L.B. Lucy, I.J. Danziger, C. Gouiffes, and P. Bouchet
European Southern Observatory, Karl-Schwarzschild-Str. 2
D-8046 Garching bei München, Federal Republic of Germany

ABSTRACT

An asymmetry of optical emission lines that appeared in Sept. 1988 is interpreted as evidence of dust condensation within the metal-rich ejecta of SN 1987A. A quantitative analysis of this spectroscopic effect is given and shown to be compatible with the photometric record. Moreover, observational and theoretical estimates of the bolometric light curve come into agreement when the far-IR excess is interpreted as thermal emission by grains in the ejecta. A grain population comprising small silicate grains with an admixture of graphite or amorphous carbon particles is suggested by the data. The relevance of this discovery to suggestions that supernovae are major sources of interstellar dust is briefly discussed.

1. INTRODUCTION

Various indirect arguments have been adduced that supernovae are major sources of interstellar dust. The initial suggestion (Cernuschi et al. 1967) that SN ejecta are promising sites for grain condensation followed from the recognition that their cooling trajectories bring about appropriate thermodynamic conditions. Subsequent consideration of the potential condensable mass per SN and of the frequency of SN led Hoyle and Wickramasinghe (1970) to note that this source alone could in ~ 10^9 yr produce the inferred mass of dust in the Galaxy. Further support for this formation site comes from the argument (Dwek and Scalo 1980; Clayton 1982) that the large depletions of refractory elements in the interstellar gas require that, when injected into interstellar space by SN explosions, these elements are already locked up in grains. The isotopic anomalies in meteorites also point to grain condensation occurring before SN ejecta are mixed and diluted with isotopically normal interstellar gas (Clayton 1982).

The prospect that SN 1987A should allow these arguments to be tested has been widely recognized, with attention focussing on the photometric consequences of dust formation. In particular, Dwek (1988) and Kozasa et al. (1989) have stressed the possibility noted already by Hoyle and Wickramasinghe (1970) of a total black-out in the UV and optical, with the SN then becoming a purely IR object. But in fact no evidence has been presented of any extinction at short wavelengths, and the observed

brightening in the IR has been interpreted as a thermal echo from pre-existing circumstellar dust (Roche et al. 1989; Felten and Dwek 1989).

In contrast, the starting point of this investigation was our recognition of a spectroscopic signature of dust within the expanding ejecta, namely the line profile asymmetry caused by the greater attenuation of radiation received from receding matter. The analogous effect in novae was first discussed by McLaughlin (1935) and is now known to appear simultaneously with the more familiar photometric signatures of dust formation (Smith et al. 1979). Chevalier (1981) has previously invoked this nova analogy when explaining an Hα asymmetry in SN 1979c as due to dust in the expanding envelope.

A brief report on this work appeared in IAUC No. 4746. The present account has been up-dated to the time of writing - late May.

2. OBSERVED PROFILES

Fig. 1 shows the change in the [OI]λ6300,6363Å profile between 5 Aug '88 and 3 Mar '89. The earlier spectrum shows the [OI] components to be essentially unshifted with respect to the LMC, whereas in the later spectrum both components are blueshifted by $\simeq$ 600 km s^{-1}.

Because this effect occurs without perturbing the secular trend in the intensity ratio of the [OI] components, it cannot plausibly be attributed to self-absorption; consequently, the blue shift must be imposed by an effect distinct from local line formation. An appealing possibility is the onset of significant attenuation within the expanding ejecta due to dust condensation. Of course, other absorption mechanisms could produce the same asymmetry; but, under the prevailing conditions of low temperature - as indicated by the prior formation of several molecular species (CO, SiO, CS) - dust is the obvious choice.

3. THEORETICAL LINE PROFILES

We take the metal-rich ejecta to be a spherically symmetric nebula (Fig. 2) expanding radially with velocity law $V = r/t$, where t is the time since core collapse. Surfaces of constant line-of-sight velocity are then simply planes $z = -v$, where the unit of length is the sphere's instantaneous radius $R_E = V_E t$ and the unit of velocity is V_E.

165

Fig. 1: Emission profile of
[OI]λ6300,6363 Å on 5 Aug '88 and
3 Mar '89. Expected wavelengths at
velocity of LMC are indicated. The
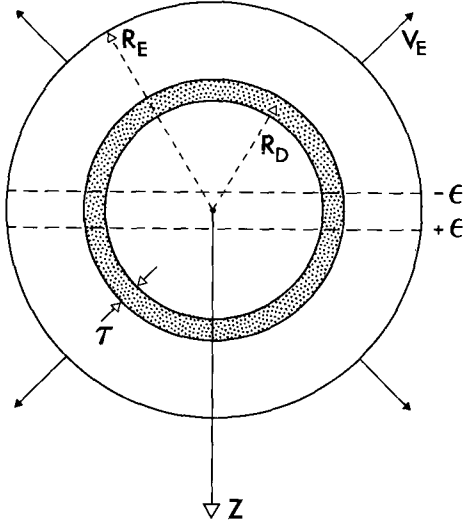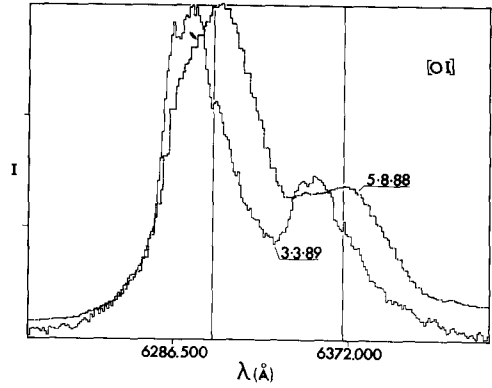profiles are scaled to same peak
intensity for violet component.

Fig. 2: Model for expanding ejecta
with dust condensation in thin shell
(Model I). The observer is at z = + ∞.

Model I. On the assumption that the spectroscopic detection of dust closely
followed its initial formation, we first suppose that dust is still restricted to a
thin spherical shell at the radius (unknown) where condensation was first allowed.
In addition, we suppose that the dust grains are still small ($2\pi a \ll \lambda$) so that dust
scattering may be neglected - i.e., the albedo $\omega \ll 1$. Now, from Fig. 2, we see
that, if the dust shell is geometrically infinitesimal, the numbers of line photons
received from planes $z = \pm \varepsilon$ become identical as $\varepsilon \to 0$. Accordingly, with $\omega = 0$, the
line profile I(v) is such that

$$\frac{dI}{dv} = 0 \quad \text{at } v = 0 , \tag{1}$$

a result that is evidently independent of τ and holds whatever the radial
distribution of line emissivity. But this prediction of zero slope at v = 0 when the
dust is in a thin shell is contradicted by the observed profiles (Fig. 1). Further

166

evidence of the poor fit of this model is provided by Fig. 3, which shows line profiles for various dust-shell radii in the case of constant line emissivity.

Model II. The obvious implication of this failure is that dust was already widely distributed when detected spectroscopically. Accordingly, retaining the assumption $\omega = 0$, we now suppose that the dust is uniformly distributed throughout the ejecta ($r < R_E$). In this case, radiation received from a point on the surface $z = +v$ is attenuated relative to that from the corresponding point on $z = -v$ by the factor $\exp(-2\tau v)$, where $\tau = k\rho R_E$. The line profile is therefore such that

$$I(v) = I(-v)\exp(-2\tau v) , \tag{2}$$

from which it follows that

$$\frac{d\ell n I}{dv} = -\tau \quad \text{at } v = 0 . \tag{3}$$

If we now make the further assumption that the line emissivity is independent of r, the blue side ($v < 0$) of the line profile is given by

$$\tau^2 I(v) = 1 - v\tau - (1+\tau)\exp\{-(1+v)\tau\} . \tag{4}$$

From this, one readily finds that maximum intensity occurs at velocity

$$v = -1 + \tau^{-1} \ell n(1+\tau) . \tag{5}$$

Examples of line profiles derived from equations (2) and (4) are given in Fig. 4.

Model III. Given that dust may have formed well before its spectroscopic detection, the possibility of large grains with non-negligible albedo must be considered. Accordingly, in Fig. 5 we present Monte Carlo calculations of line profiles for uniform distributions of line emissivity and dust, with the dust grains now being isotropic scatterers with $\omega = 0.6$, an albedo typical of local Galactic dust in the visual (Witt 1988). These profiles reveal a potentially useful diagnostic for dust scattering in the form of an extended red wing comprising photons that escape after several scatterings. These photons are redshifted because they have done work on the expanding sphere of dust.

4. ANALYSIS OF OBSERVED LINE PROFILES

The above simple models can be used to quantify the amounts and other properties of the dust required by our explanation of the line profile asymmetry. If this
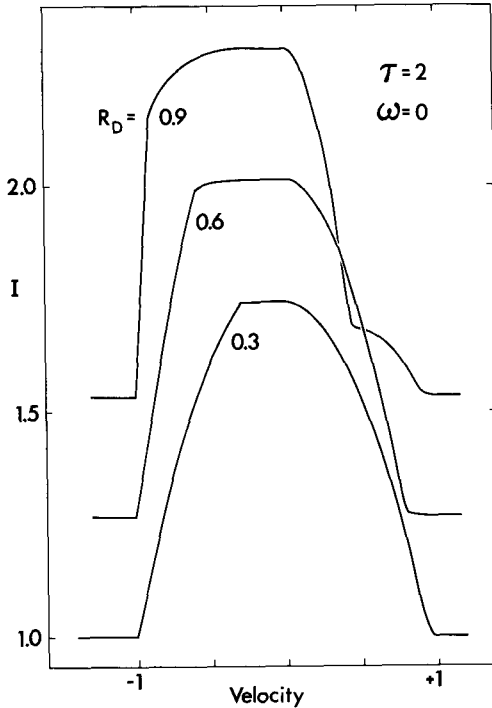
167

Fig. 3: Theoretical line profiles for Model I. Thin shells of zero-albedo dust with τ = 2 at various radii R_D. Line emissivity is constant.
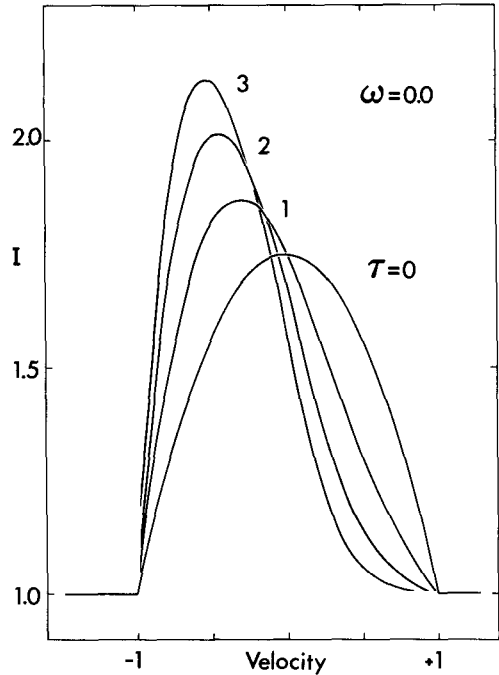
Fig. 4: Theoretical line profiles for Model II. Zero-albedo dust uniformly distributed in the ejecta with various values of $τ = kρR_E$. Line emissivity is constant.

spectroscopically derived data proves compatible with the photometric record, the dust condensation hypothesis will be greatly strengthened, and a more sophisticated modelling of the line profiles will then be justified.

Albedo. The diagnostic of dust scattering exhibited in Fig. 5 is not convincingly seen when line profiles before and after dust condensation are compared. However, because of the difficulty of defining a continuum, the predicted effect for ω = 0.6 is roughly the limit of what could in fact be detected. Accordingly, we conclude that ω ≲ 0.6 in the interval λλ4600-9800Å. If we now model the dust with a single particle species and size, this albedo limit implies a grain radius a ≲ 0.05 μ for grains of "astronomical silicate" (Draine and Lee 1984). But for grains of iron (Wickramasinghe 1973) or graphite (Draine and Lee 1984), the albedo limit is not sufficiently restrictive to limit particle sizes. Because of the non-detection of this albedo effect, we subsequently take ω = 0.
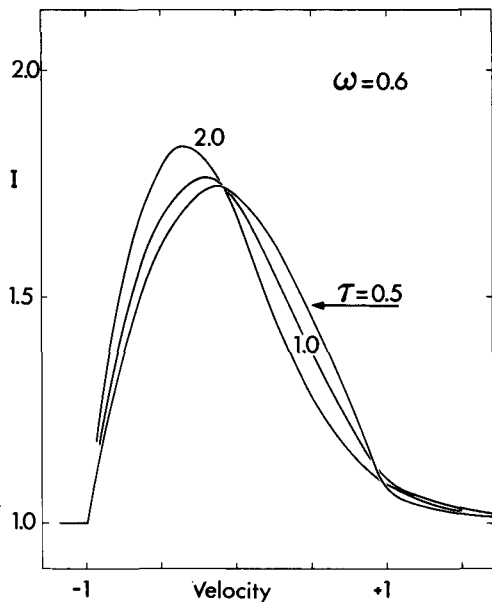
168

Fig. 5: Theoretical line profiles for Model III. Dust with albedo = 0.6 is uniformly distributed through the ejecta with indicated values of $\tau = k\rho R_E$.
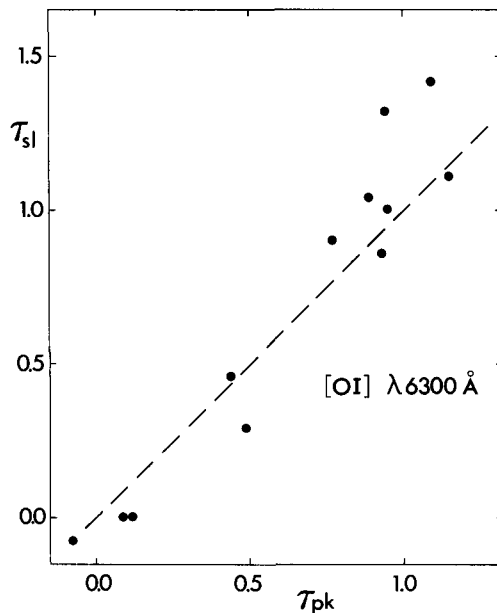
Fig. 6: Comparison of independent estimates of $\tau = k\rho R_E$ for Model II from observed [OI]λ6300 Å profile.

Expansion Velocity. With $\omega = 0$ and uniform distributions of dust and line emissivity (Model II), line profiles $I(\lambda)$ depend on two parameters V_E and τ. We now determine V_E by requiring that the parabolic profile predicted when $\tau = 0$ has the same half width at half intensity as does the violet side of the [OI]λ6300Å line before dust condensation. From measurements on three spectra, we thus obtain $V_E = 1870$ km s^{-1}, a value used throughout the remainder of this investigation.

Distribution of Dust. In Sect. 3, we noted the superiority of line profiles computed under the assumption of a uniform distribution of dust (Model II) as against the thin-shell model (Model I). This can be tested quantitatively by comparing τ_{sl} and τ_{pk}, independent estimates of $\tau = k\rho R_E$ that can be derived from an observed profile by application of equations (3) and (5), respectively. This comparison is shown in Fig. 6 for the [OI]λ6300Å line. (Note that here and below negative values of τ have been accepted.)

Because Fig. 6 reveals that $\tau_{sl} \propto \tau_{pk}$ and because the thin-shell model predicts $\tau_{sl} = 0$, we conclude that, when spectroscopically detected via blue shifts, dust was already widely distributed in the ejecta. Nevertheless, since simultaneous condensation throughout the ejecta is implausible, a more refined analysis of line profiles might well yield earlier evidence of dust within a restricted range of

169

Fig. 7: Optical depth τ_λ as function of time t derived from blue shifts of indicated lines using Eq.(5).
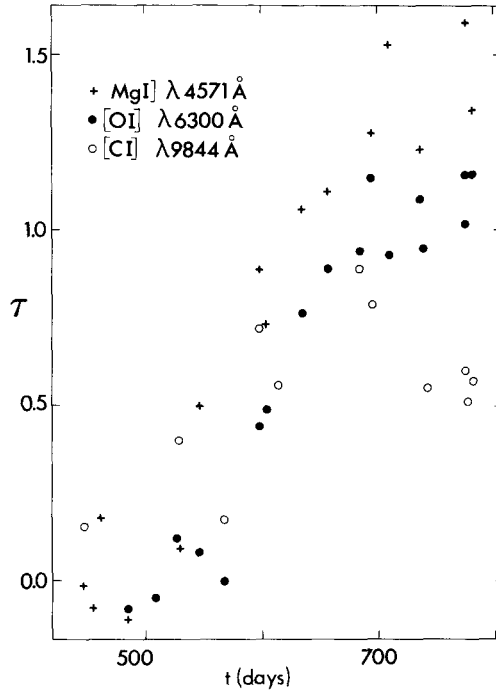
radii. In view of the successful outcome of this test, Model II is used throughout the remainder of this paper.

Evolution of τ_λ. Model II is now used to derive the dependence of $\tau = k\rho R_E$ on both time and wavelength from the varying blue shifts of different lines. The lines measured are: MgI]λ4571Å, [OI]λ6300Å, and [CI]λ9844Å. For the unblended Mg and O lines, τ_λ is given directly by Eq. (5). For the C line, which is a triplet with overlapping components, the corresponding τ_λ is obtained by assuming the individual components' profiles are given by Eqs. (2) and (4) with intensities proportional to their respective Einstein A coefficients. The resulting values of τ_λ are plotted against t in Fig. 7. Unfortunately, the spectra from which·these data derive are not of uniform S/N. As is evident from the scatter, the OI measures are the most, and the CI the least, reliable. The four CI measures after t = 740d are, however, of greater weight than the earlier CI data.

Inspection of the OI data suggests that the dust optical depth in the ejecta has been a smooth and monotonically increasing function of time, being negligible prior to t ≈ 530d, increasing rapidly after t ≈ 580d, and then only slowly after t ≈ 670d.

Fig. 6 also reveals clear evidence of selective extinction, especially when low weight is assigned to the CI measures prior to t = 740d. The observed increase in τ_λ

with decreasing λ requires that extinction in the optical is <u>not</u> dominated by large grains. Using the same sources as above, we find that these data imply a ≲ 0.5µ for grains of astronomical silicate, and a ≲ 0.1µ for either graphite or iron. Note that the silicate limit is less restrictive than that derived from the albedo diagnostic.

For later testing of compatibility with photometric data, it is useful to derive the optical depth $\tau_v(t)$ at λ = 5500Å, the effective wavelength of the V band. This has been done by fitting a smooth curve to the OI data and then correcting to 5500Å by assuming that $\tau_\lambda \propto \lambda^{-1}$, a formula roughly consistent with the MgI data. The resulting values are given in Table I, together with the implied mean extinction $A_v = -2.5 \log p$, where $p(\tau_v)$ is the escape probability. Under the assumptions of Model II, Osterbrock's (1974, p.242) formula for p applies.

Table 1
Optical depth and mean extinction at λ = 0.55µ

t(dys)	τ_v	A_v(mag.)	t(dys)	τ_v	A_v(mag.)
500	0.00	0.00	650	0.97	0.68
525	0.02	0.02	675	1.08	0.74
550	0.08	0.06	700	1.15	0.78
575	0.21	0.17	725	1.19	0.80
600	0.54	0.40	750	1.22	0.82
625	0.81	0.58	775	1.25	0.84

<u>Condensation Efficiency</u>. On the assumption that the grains are all of the same size and composition, the dust mass required by Model II to produce optical depth τ_v is

$$M_d = \frac{16}{9} \pi R^2 \frac{\rho a}{Q_v} \tau_v \ , \tag{6}$$

where ρ is the density of the grains and $Q_v(a)$ is their extinction efficiency at λ = 0.55µ. For small grains, $Q \propto a$ and so M_d is then independent of a. Note also that when grain condensation stops τ_v decreases as t^{-2}.

Because the spectroscopic data on blue shifts does not decisively favour a particular grain composition, we apply Eq. (6) to several plausible candidates. At t = 775d, the end of the reported observing period, the still increasing grain masses are: 3.2×10^{-4}, 6.7×10^{-5}, 1.6×10^{-5}, and 4.4×10^{-6} solar masses for small grains of astronomical silicate, iron, graphite, and amorphous carbon, respectively. The requisite grain properties were obtained from the sources cited earlier, except for amorphous carbon where the Rowan-Robinson and Harris (1983) fit to the experimental data of Koike et al. (1980) was used.

171

Using the abundances predicted for the ejecta by Hashimoto et al. (1989), we can compute the maximum mass possible for grains of a given composition and thus convert the above grain masses into condensation efficiencies. The resulting efficiencies up to t = 775d are 6.2×10^{-4}, 8.1×10^{-4}, 1.4×10^{-4} and 3.9×10^{-5} for grains of astronomical silicate, iron, graphite and amorphous carbon, respectively. The result for astronomical silicate derives from a maximum mass of 0.51 M_O obtained by assuming it to be Mg_2SiO_4. At first sight, these low efficiencies suggest that far more condensation will occur in the coming months and that the predicted black out might yet occur. Another possibility, however, is that the condensation efficiency is already much higher but is not evident because of the clumpiness of the dust distribution.

5. ADDITIONAL SPECTROSCOPIC EVIDENCE

Dust absorption may also explain the weakening of the $[CoII]\lambda 10.5\mu$ line below its predicted strength. At t = 280 and 400d, this line was observed (IAUC No. 4575) at the strengths expected from the decay of an initial 0.075 M_O of ^{56}Ni. But at t = 638d, its strength was only 0.37 of that predicted - this calculation assumes an ionization ratio CoII:CoI of 1:2, which is supported by observations of FeII and FeI lines. If this deficiency is indeed due to dust absorption, then τ_λ = 1.8 at 10.5μ at an epoch when τ_λ = 0.9 at 0.55μ - see Table I. On the assumption of a single grain species, this gives $Q(10.5\mu)/Q(0.55\mu)$ = 2.0. For small grains of astronomical silicate, this ratio is 1.85. But for graphite and amorphous carbon this ratio is 0.011 and 0.052, respectively; and graphical data given by Wickramasinghe (1973) indicates that this ratio is $\le$ 0.01 for Fe. This appears to be a decisive argument in favour of silicate grains, but its crucial dependence on the ionization ratio of cobalt must be noted.

Depletion. In Sect. 4, we found the condensation efficiency to be low but remarked that clumpiness allows higher values. If the condensation efficiency were in fact to approach unity for some grain species, then the depletion of the least abundant contributing element might become evident spectroscopically. At first sight, an observed weakening after day 550 of the $[SiI]\lambda 1.64\mu$ line relative to the continuum suggests depletion, and this would strongly support silicate as the dominant grain species. However, this line is temperature sensitive, and so the observed effect may simply be due to declining excitation in the cooling ejecta. Clearly, independent and accurate temperature estimates are needed before depletion can be claimed.

172

6. PHOTOMETRIC EVIDENCE - OPTICAL

We now test our interpretation of the line profile asymmetry by examining its compatibility with the photometric record.

Extinction. In their analysis of the superb Geneva photometry of SN 1987A, Burki et al. (1989) do not invoke extinction when interpreting the behaviour of the V light curve up to t = 700d. Moreover, Roche et al. (1989), in favouring time-delayed emission from pre-existing circumstellar grains - a thermal echo - when explaining their IR observations on day 580, exclude prompt emission from newly created grains within the ejecta in part because the concomitant optical extinction is not seen. Nevertheless, Fig. 8 shows that, when corrected for the slowly increasing mean visual extinction (Table I) derived from our analysis of the McLaughlin effect, the resulting dust-free V light curve is not implausible: it shows the expected (e.g. Pinto et al. 1988) monotonically increasing departure from the earlier exponential decay in consequence of the ejecta's increasing transparency to γ-rays.

Note that the corrected light curve shows no evidence of energy input from the pulsar (cf. Burki et al. 1989). On our interpretation, the slowing decline of the observed V light curve after $\simeq$ day 650 is due to a slowing in the rate of dust condensation.

Fluctuations. Burki et al. (1989) have called attention to variability on a time scale shorter than roughly 10-20 days of the U and B light curves after day 450 and note that the V curve is more stable. This short time scale implicates the ejecta, and the coincidence of its onset with the brightening at 10μ (IAUC No. 4645; Roche et al. 1989) suggests dust. A possible interpretation is as follows: The continuum is emitted by discrete clumps, some of which after day 450 are occulted by dust clouds. These clouds are relatively opaque in the U band and relatively transparent in the V band. Light curve spikes occur when a clump emerges from occultation - as when the sun suddenly shines through a gap in the clouds. This interpretation is qualiatively consistent with our suggestion (Sect. 4) that dust condensation might have started well before it became evident via the McLaughlin effect.

7. PHOTOMETRIC EVIDENCE - INFRARED

The AAT Experiment. As noted earlier, Roche et al. (1989) attribute the 10μ excess to a thermal echo. The principal reason for this preference was their discovery that SN 1987A had a measurable angular size at 8-10μ on day 580. Specifically, they measured a FWHM of 2$\overset{''}{.}$2 for the supernova as against 1$\overset{''}{.}$6 for comparison stars. But they also found the IR profiles to be centred on the supernova to within 0$\overset{''}{.}$25.

173

Accordingly, while convincingly establishing a contribution from distant dust, their experiment does not exclude models that assign a substantial fraction of the 10μ emission to dust within the ejecta.

IR Emission from the Ejecta. In computing IR emission from dust within the ejecta, we again adopt Model II from Sect. 3. Thus we suppose the dust to be uniformly distributed in (0,R) and to have $\omega = 0$. In addition, we assume the emissivity of the gas to be constant for $r < R$ and zero for $r > R$. With this model, we calculate as a function of t the maximum amount of dust of a given type permitted by the photometric record. The steps in the calculation are the following:

A) Specify t and choose grain model - e.g. graphite with a = 0.01μ.
B) Guess $\tau_V(t)$, the optical depth $k\rho R$ at 0.55μ.
C) From τ_V and the known function $Q_\lambda(a)$, compute τ_λ and hence the escape probabilities $p_\lambda = p(\tau_\lambda)$ at the effective wavelengths of the photometric bands.
D) Derive the generated luminosity density $\Lambda_\lambda^d + \Lambda_\lambda^g$ due to emission by dust and gas from the observed luminosity density L_λ via the equation

$$ L_\lambda = p_\lambda (\Lambda_\lambda^d + \Lambda_\lambda^g) \ . \tag{7} $$

E) Assume an isothermal stratification for the dust. The dust's temperature may then be derived iteratively from the condition of its global thermal equilibrium,

$$ \int (1-p_\lambda)(\Lambda_\lambda^d + \Lambda_\lambda^g) d\lambda = \int \Lambda_\lambda^d \ d\lambda \ . \tag{8} $$

F) With Λ_λ^d now determined, Eq. (7) is solved for Λ_λ^g.
G) If $\Lambda_\lambda^g > 0$ at all λ, then τ_V is increased and steps C)-F) are repeated.
H) A converged model has $\Lambda_\lambda^g = 0$ at some λ.

The photometric record used for these calculations comprises broad band light curves, smoothed and read off at 25 day intervals. The raw data at short wavelengths - $UBVR_cI_c$ - is from the South African observers (Whitelock et al. 1989, and references therein), while at longer wavelengths - $JHKLMN_1N_2N_3Q_0$ - the data is from ESO La Silla. The quantities $L_\lambda(t)$ were derived from the photometric magnitudes using LMC distance modulus = 18.5 and after correcting for foreground extinction assuming E(B-V) = 0.15.

The maximum permitted τ_V's as a function of time are plotted in Fig. 9 for the grain species considered earlier (Sect. 4), all for a = 0.01μ, as well as for grey particles ($Q_\lambda \equiv 1$). Also shown is $\tau_V(t)$ derived spectroscopically (Table I). These results show that the $\tau_V(t)$ functions for small silicate grains and for grey
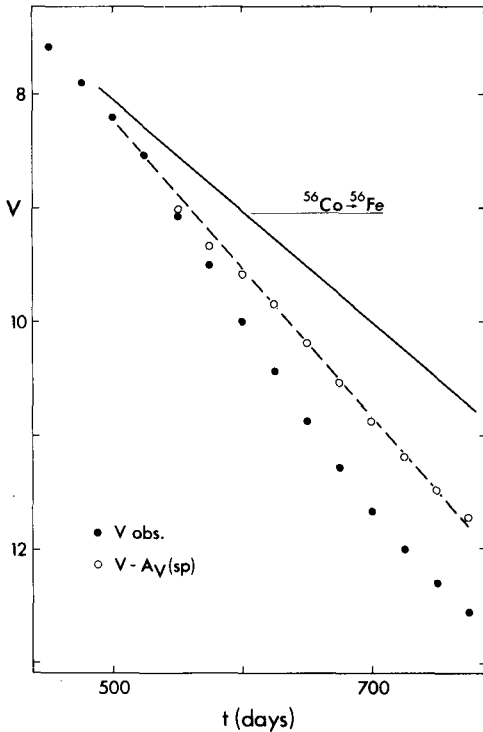
174

Fig. 8: Visual light curve corrected for extinction by internal dust. The spectroscopically derived correction $A_v(Sp)$ is from Table I. The observed points are a smoothed version of South African data (Sect. 7).
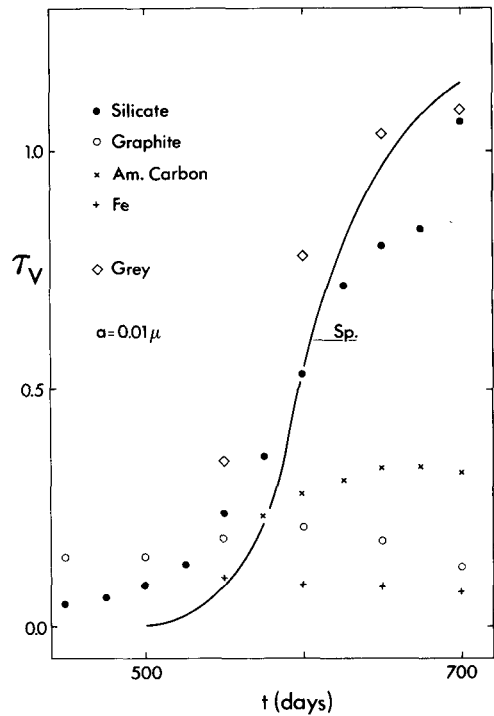
Fig. 9: Maximum optical depth τ_v at 0.55μ for different grain species, all for a = 0.01μ. Also plotted is the spectroscopically-derived τ_v from Table I.

particles track the spectroscopic function rather well. But this is not true for small grains of graphite, amorphous carbon, or iron; and so small grains of these substances can only be minor constituents of the ejecta's dust population. Of course, large grains of any substance approximate grey absorbers and so would be admitted as major constituents by this photometric argument. But the spectroscopic evidence of selective extinction in the optical (Sect. 4; Fig. 7) forbids this.

The differences in maximum τ_v's between the various grain species (and sizes) are due to differences in emission efficiencies in the far-IR. This is illustrated in Fig. 10 where emission by silicate and graphite grains with a = 0.01 μ is compared with the photometric data on day 625. The silicate grains, being efficient radiators, have low equilibrium temperature T_d = 356K and are limited to τ_v = 0.72 by the flux in the N_2 band (λ_{eff} = 9.69μ). For graphite grains, on the other hand, low emission efficiency requires T_d = 676K and they are limited to τ_v = 0.20 by the flux in the L band (λ_{eff} = 3.78μ). Fig. 10 also shows the effect on the silicate

175

emission of dust in the ejecta being clumped with filling factor $\alpha = 0.1$ and with the individual blobs having $\tau_b = k\rho R_b = 3$. Further details of such calculations will be given elsewhere.

Fig. 9 perhaps suggests that compatibility of the spectroscopic and photometric data can be achieved simply by assuming all the grains to be small silicate particles. But this would not allow 10μ emission from distant dust, as required by the AAT experiment. Fortunately, a mixture satisfying this further constraint can be constructed: On day 625, spectroscopy (Table I) requires $\tau_v = 0.81$, which is fulfilled if we assign $\tau_v = 0.55$ to silicates and 0.26 to amorphous carbon. This choice allows ≈ 24% of the 10μ emission to be attributed to circumstellar dust, an amount probably consistent with the AAT experiment. If graphite is preferred as the minor constituent, the silicate contribution must increase to $\tau_v = 0.61$, and only 15% of the 10μ emission is then circumstellar. These simple exercises show that the dust condensation hypothesis can satisfy the observational constraints and that it does so with an astrophysically plausible mix of grain types and sizes.

The above results are somewhat in conflict with work of Moseley et al. (1989). These authors in analyzing data from days 623 and 639 conclude that emission from graphite particles with $a = 0.1\mu$ and $T_d \sim 300\text{-}400K$ dominates the IR continuum from 18-35μ and suggest that this is the newly-formed dust that we inferred (IAUC No. 4746) from line profile asymmetries. However, for graphite grains in the ejecta, our calculations give $T_d = 693K$ on day 625 for $a = 0.1\mu$ and thus negligible emission for $\lambda > 10\mu$ - cf. Fig. 10. If their radii are increased to $a = 1\mu$, T_d drops to 406K and then the far IR can indeed be accounted for. But then the near perfect greyness of such particles at short wavelengths is incompatible with the inferred selective extinction in the optical (Sect. 4; Fig. 7).

8. PHOTOMETRIC EVIDENCE - BOLOMETRIC

Pinto et al. (1988) have stressed that, because of the simplicity of the physics of the transfer and degradation of γ-rays in the SN's envelope, the prediction of the luminosity generated by the thermalization of γ-rays emitted by ^{56}Co and ^{57}Co is reliable, given their initial radial distribution. They therefore emphasized the diagnostic possibilities of such calculations for detecting departures from a model in which the "bolometric" light curve (excluding X- and γ-rays) is powered solely by promptly thermalized input from unstable isotopes.

In the present context, this diagnostic is of interest for testing whether the far-IR excess is due predominantly to newly-formed dust in the ejecta or to pre-existing circumstellar dust. In the former case, the IR excess represents prompt
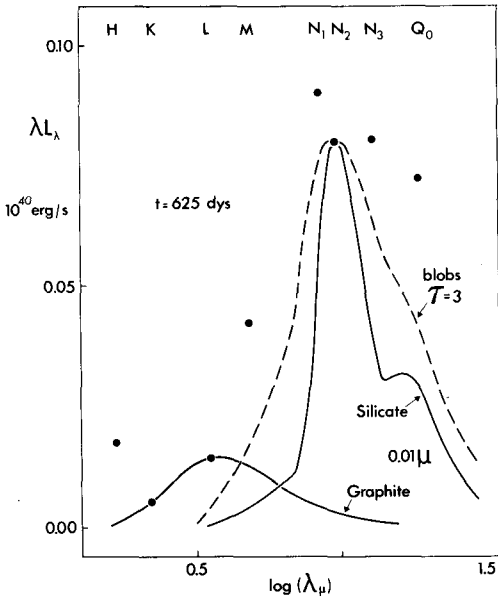
176

Fig. 10: Grain emission on day 625. Maximum emission by silicate and graphite grains with a = 0.01μ is shown together with photometric data. Effect of clumping on silicate emission is also shown.
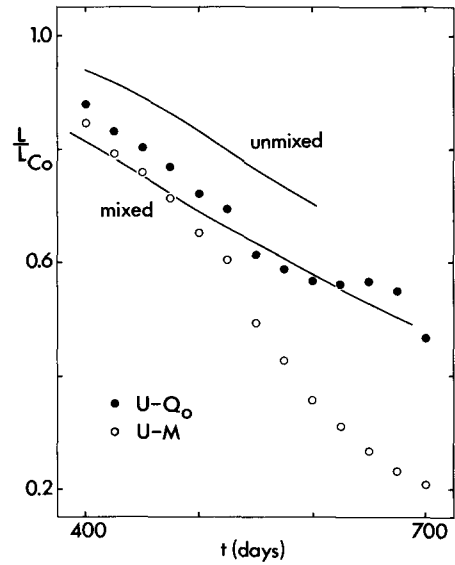
Fig. 11: Bolometric emission as fraction of energy released by ^{56}Co. Effect on observational estimates including (U-Q_0) and excluding (U-M) far-IR is shown. Theoretical calculations from Pinto et al. (1988).

emission and so must be included in estimating the bolometric luminosity. But in the latter case, the IR excess is a thermal echo of radiation emitted at $\simeq$ t - 400 days and so must be excluded.

These two alternative observational estimates of the bolometric luminosity are compared with the Pinto et al. (1988) calculations in Fig. 11. The 14 broad-band light curves identified in Sect. 7 are again used and the IR excess whose origin is in question is defined as the flux in the N_1-Q_0 bands. (The quadrature formula used here and for the integrals in Eq.[8] has end-point weights derived by assuming black body emission at T = 2000K for λ < 0.4μ and emission from grains with Q $\propto \lambda^{-2}$ for λ > 20μ.) Fig. 11 shows that assigning the IR excess to the ejecta gives a bolometric light curve that agrees well with the preferred model ("mixed") of Pinto et al. (1988). Accordingly, this test provides strong support for the dust condensation hypothesis. Interestingly, it also supports our earlier suggestion (Sect. 7) that only a modest percentage ($\lesssim$ 25%) of the IR excess derives from circumstellar dust.

That L(U-M) had begun to fall below model predictions was first pointed out by Catchpole et al. (1988), and they noted the possibility of significant flux at other

wavelengths. More recently, Moseley et al. (1989) have used their far-IR observations to discuss the SN's energy budget on day 613 and find this to be balanced if the IR excess is attributed to dust in the ejecta.

Some structure is evident in the $L(U-Q_0)$ bolometric light curve in Fig. 11. If not due to quadrature errors, this could be due to departures from simultaneity in dust condensation in a given spherical shell. This would result in a failure of the instantaneous balancing of optical extinction and IR excess. The thermal echo is of course a further complication.

9. CONCLUSION

The aim of this investigation has been to collect and analyze evidence relating to the possible condensation of dust in the metal-rich ejecta of SN 1987A. In view of the number of independent supporting arguments as well as their mutual consistency, both quantitative and chronological, we conclude that dust has indeed formed in the ejecta.

In thus establishing that dust can in fact form in the ejecta of Type II supernovae, we have added direct observational support to the indirect arguments summarized in Sect. 1 that identify supernovae as major sources of interstellar dust. Moreover, our crude initial attempt to determine the mix of grain species is not inconsistent with this hypothesis. However, on the negative side, our estimates of the condensation efficiencies fall short by factors $\geq 10^2$ of those demanded by this hypothesis, which therefore requires that the bulk of the grain formation lies in the future. Moreover, there is the question of the dust's survival when a reverse shock slows the ejecta's expansion. Perhaps a new phase of dust condensation follows this event or perhaps the surviving grain fragments reaccrete refractory elements immediately after the shock's passage (Seab 1987). If this phase of grain formation or growth goes to completion before mixing occurs across the contact discontinuity, then the observational constraints summarized in Sect. 1 are met.

178

REFERENCES

Burki, G., Cramer, N., Burnet, M., Rufener, F., Pernier, B., Richard, C.: 1989, Astron. Astrophys. 213, L26

Catchpole, R.M., Whitelock, P.A., Menzies, J.W., Feast, M.W., Marang, F., Sekiguchi, K., van Wyk, F., Roberts, G., Balona, L.A., Egan, J.M., Carter, B.S., Laney, C.D., Laing, J.D., Spencer Jones, J.H., Glass, I.S., Winkler, H., Fairall, A.P., Lloyd Evans, T.H.H., Cropper, M.S., Shenton, M., Hill, P.W., Payne, P., Jones, K.N., Wargau, W., Mason, K.O., Jeffery, C.S., Hellier, C., Parker, Q.A., Chini, R., James, P.A., Doyle, J.G., Butler, C.J., Bromage, G.: 1989, Monthly Notices Roy. Astron. Soc. 237, 55P

Cernuschi, F., Marsicano, F., Codina, S.: 1967, Ann. d'Astrophys. 30, 1039

Chevalier, R.A.: 1981, Astrophys. J. 251, 259

Clayton, D.D.: 1982, Q.J. Roy. Astron. Soc. 23, 174

Draine, B.T., Lee, H.M.: 1984, Astrophys. J. 285, 89

Dwek, E., Scalo, J.M.: 1980, Astrophys. J. 239, 193

Dwek, E.: 1988, Astrophys. J. 329, 814

Felten, J.E., Dwek, E.: 1989, Nature 339, 123

Hashimoto, M., Nomoto, K., Shigeyama, T.: 1989, Astron. Astrophys. 210, L5

Hoyle, F., Wickramasinghe, N.C.: 1970, Nature 226, 62

Koike, C., Hasegawa, H., Manabe, E.: 1980, Astrophys. Sp. Sc. 67, 495

Kozasa, T., Hasegawa, H., Nomoto, K.: 1989, Astrophys. J. (in press)

McLaughlin, D.B.: 1935, Pub. Am. Astron. Soc. 8, 145

Moseley, S.H., Dwek, E., Glaccum, W., Graham, J.R., Loewenstein, R.F., Silverberg, R.F.: 1989, Nature (in press)

Osterbrock, D.E.: 1974, Astrophysics of Gaseous Nebulae (W.H. Freeman; San Francisco)

Pinto, P.A., Woosley, S.E., Ensman, L.M.: 1988, Astrophys. J. 331, L101

Roche, P.F., Aitken, D.K., Smith, C.H., James, S.D.: 1989, Nature 337, 533

Rowan-Robinson, M., Harris, S.: 1983, Monthly Notices Roy. Astron. Soc. 202, 797

Seab, C.G.: 1987, Interstellar Processes, eds. D.J. Hollenbach and H.A. Thronson, Jr. (Reidel), p.491

Smith, S.E., Noah, P.V., Cottrell, M.J.: 1979, Pub. Astron. Soc. Pac. 91, 775

Whitelock, P.A., Catchpole, R.M., Menzies, J.W., Feast, M.W., Woosley, S.E., Allen, D.A., van Wyk, F., Marang, F., Laney, C.D., Winkler, H., Sekiguchi, K., Balona, L.A., Carter, B.S., Spencer Jones, J.H., Laing, J.D., Lloyd Evans, T., Fairall, A.P., Buckley, D.A.H., Glass, I.S., Penston, M.V., da Costa, L.N., Bell, S.A., Hellier, C., Shara, M., Moffat, A.F.J.: 1989, Monthly Notices Roy. Astron. Soc. (in press)

Wickramasinghe, N.C.: 1973, Light Scattering Functions for Small Particles, (Adam Hilger; London)

Witt, A.N.: 1988, Dust in the Universe, eds. M.E. Bailey and D.A. Williams (Cambridge University Press), p.1

Discussion:

CESARSKY, C.: The minimum rate of grain condensation corresponds to the case of uniform distribution - no clumpling. What is this rate for SN1987a.

LUCY: In the printed text, the masses and condensation efficiencies refer to the uniform distribution model and are therefore the minimum value you request.

BECKER: Fesen and I have recently taken spectra of SN1980k eight years after maximum. The emission lines show a strong assymetry, consistent with the formation of dust in the ejecta.

LUCY: I noted with interest you recent account of these spectra in BAAS. I believe that you are indeed observing the same phenomenon that we have described for SN1987a.